Biferrocene-Based Diphosphine Ligands: Synthesis and Application of Walphos Analogues in Asymmetric Hydrogenations

Afrooz Zirakzadeh,[†] Manuela A. Groß,[†] Yaping Wang,[‡] Kurt Mereiter,[§] Felix Spindler,[||] and Walter Weissensteiner*,[†]

[†]Institute of Organic Chemistry, University of Vienna, Währinger Straße 38, A-1090 Wien, Austria

[‡]College of Pharmaceutical Sciences, Capital Medical University, Beijing, No. 10 Xitoutiao, You An Men Beijing 100069, People's Republic of China

[§]Institute of Chemical Technologies and Analytics, Vienna University of Technology, Getreidemarkt 9/164SC, A-1060 Vienna, Austria

[||]Solvias AG, Synthese & Katalyse, Römerpark 2, CH-4303 Kaiseraugst, Switzerland

S *Supporting Information*

ABSTRACT: A total of four biferrocene-based Walphos-type ligands have been synthesized, structurally characterized, and tested in the rhodium-, ruthenium- and iridium-catalyzed hydrogenation of alkenes and ketones. Negishi coupling conditions allowed the biferrocene backbone of these diphosphine ligands to be built up diastereoselectively from the two nonidentical and nonracemic ferrocene fragments (R)-1-$(N,N$-dimethylamino)ethylferrocene and (S_{Fc})-2-bromoiodoferrocene. The molecular structures of (S_{Fc})-2-bromoiodoferrocene, the coupling product, two ligands, and the two complexes ($[PdCl_2(L)]$ and $[RuCl(p\text{-cymene})(L)]PF_6$) were determined by X-ray diffraction. The structural features of complexes and the catalysis results obtained with the newly synthesized biferrocene-based ligands were compared with those of the corresponding Walphos ligands.
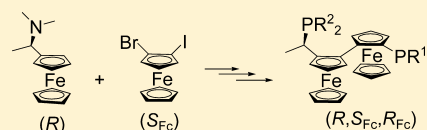
INTRODUCTION

Biaryl-based diphosphines such as 2,2′-bis-(diphenylphosphino)-1,1′-binaphthyl (BINAP) belong to the most widely and most successfully used catalyst ligands in asymmetric catalysis.[1] Since Noyori's pioneering work on the synthesis and application of BINAP,[2] this field has seen enormous development. Numerous investigations have been carried out with the aim of making structural variations and identifying further applications of BINAP. For this purpose the binaphthyl unit has been replaced by other biaryl backbones, the phosphine substituents have been varied, and spacers between the biaryl backbone and phosphine units have been introduced. From these attempts a variety of BINAP analogues have evolved and many of these have been applied successfully in asymmetric catalysis.[3]

Ito later investigated ligands that contain a biferrocene rather than a biaryl backbone, and in 1991 he reported the C_2-symmetric BIFEP ligand[4] and the TRAP ligand[5] family (Chart 1). As an extension of this concept, P-chiral[6] and unsymmetrically substituted BIFEP ligands[7] were investigated. Interestingly, and in contrast to BINAP, the use of BIFEP ligands for asymmetric hydrogenations resulted in only moderate product ee's. This fact was attributed to the conformational flexibility of the biferrocene backbone, which is able to rotate around the biferrocene axis even on coordination to transition metals.[7b] In contrast to BIFEP, TRAP-type ligands performed excellently when used in asymmetric hydrogenations. This behavior was noted with surprise, as TRAP ligands preferentially adopt a

Chart 1
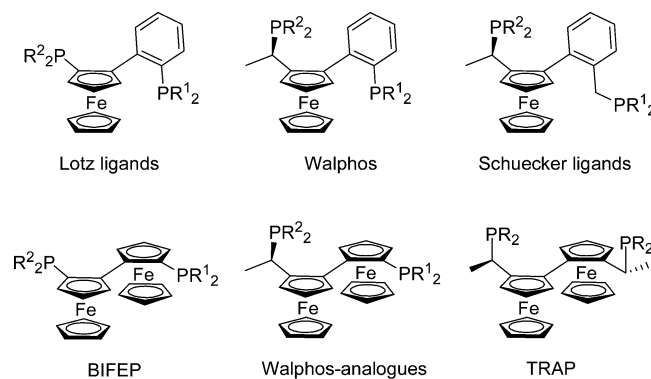
trans rather than a *cis* geometry when coordinated to transition metals.[5c,8]

A few years later, ligands having a ferrocenyl–aryl backbone were investigated. In 2002 Lotz and Knochel reported on ferrocenyl–aryl-based BINAP/BIFEP analogues (Chart 1, Lotz ligands) but, similarly to BIFEP, only moderate to good product ee's were obtained in asymmetric hydrogenations.[9] Replacement of the biferrocene backbone of TRAP ligands by a ferrocenyl–aryl unit (Chart 1, Schuecker ligands) also gave *trans*-coordinating ligands, which in the hydrogenations of

Scheme 1

[Pd]: [Pd$_2$(dba)$_3$]CHCl$_3$; tfp: tri(2-furyl)phosphine
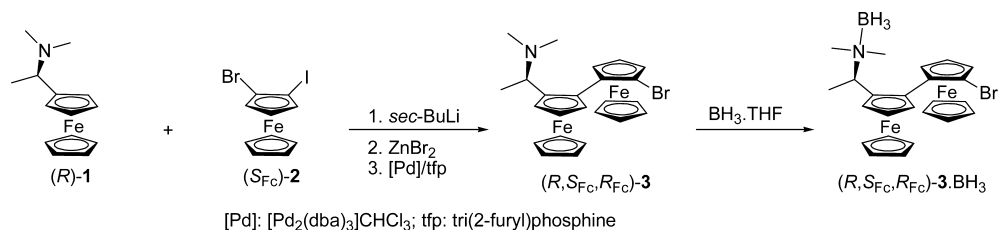
alkenes gave acceptable to excellent results—albeit with a rather limited scope of substrates.[10]

Like many other ferrocene-based diphosphine ligand systems,[11] the Walphos ligand family had originally been developed with asymmetric hydrogenations in mind.[12] On complexation with transition metals these ligands form eight-membered chelate rings and the ligand is coordinated *cis* to the metal. Applications in rhodium- and ruthenium-catalyzed asymmetric hydrogenation of olefins and ketones resulted in product enantioselectivities of up to 95% and 97%, respectively.[12] Since one Walphos-type ligand proved to be highly suitable for the asymmetric hydrogenation of a 2-isopropylcinnamic acid derivative,[12b] an intermediate in the synthesis of the renin inhibitor Aliskiren, these ligands were commercialized and are now available on a technical scale. In addition to hydrogenations,[13] including cluster-based hydrogenations,[14] Walphos-type ligands were successfully applied in a number of other enantioselective catalytic reactions such as cycloadditions,[15] coupling reactions,[16] copper hydride mediated reactions,[17] and others.[18] While originally developed as a potential alternative to BINAP, the Walphos ligand family is now considered a privileged class of ligands in its own right and searches for novel applications are still continuing. On the basis of the success of these ligands, we questioned whether Walphos analogues with a biferrocene instead of a ferrocenyl—aryl backbone could be synthesized and were curious as to how they would perform in asymmetric catalysis. It is clear that such an approach would not only result in a novel class of catalyst ligands but would also bridge the structural gap between BIFEP- and TRAP-type ligands.

We report here the synthesis of four biferrocene-based Walphos analogues and their application in the rhodium-, ruthenium-, and iridium-catalyzed hydrogenation of alkenes and ketones. A comparison of the results obtained with the newly synthesized ligands and those of the corresponding Walphos ligands is also discussed. This comparison concerns the structural features of ligands, two of their palladium and ruthenium complexes, and the hydrogenation results.

■ RESULTS AND DISCUSSION

Synthesis of Ligands and Complexes. In analogy to our previously reported Walphos synthesis,[12] a Negishi coupling of (*R*)-1-(*N*,*N*-dimethylamino)ethylferrocene ((*R*)-**1**) with 2-bromoiodoferrocene was attempted (Scheme 1). This approach should ensure the high modularity of the original synthesis route and should allow the phosphine units to be varied easily and independently. It is clear, however, that a coupling reaction between (*R*)-**1** and racemic 2-bromoiodoferrocene would lead to two coupling products, (*R*,*S*$_{Fc}$,*R*$_{Fc}$)-**3** and its diastereomer (*R*,*S*$_{Fc}$,*S*$_{Fc}$)-**3**. Therefore, in order to synthesize either of these derivatives diastereoselectively, enantiomerically pure (*R*$_{Fc}$)- or (*S*$_{Fc}$)-**2** was needed.[19]

Enantiopure (*S*$_{Fc}$)-**2** could be obtained by applying Kagan's sulfoxide methodology.[20] It is well-known not only that *p*-tolylsulfinyl units direct diastereoselectively to *ortho* positions but also that they can be exchanged with other electrophiles, even when positioned next to a tributylstannyl unit. Therefore, (*R*,*S*$_{Fc}$)-2-(*p*-tolylsulfinyl)-tributylstannylferrocene ((*R*,*S*$_{Fc}$)-**4**)[20] was treated with *t*-BuLi at −78 °C and added to a solution of tetrabromoethane (Scheme 2).

Scheme 2
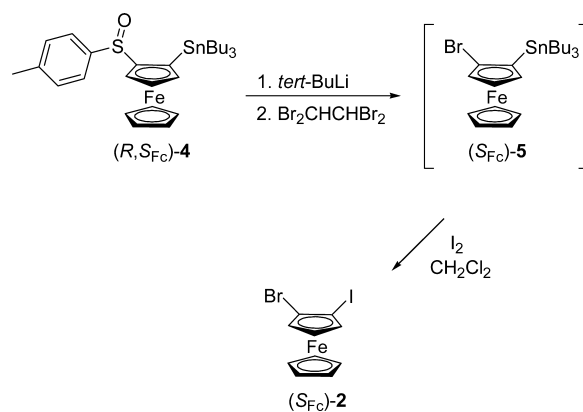
This resulted in a mixture of the desired product (*S*$_{Fc}$)-**5** and tributylstannylferrocene in a ratio of 87:13. The mixture could not be fully separated by chromatography. Treatment of this mixture with iodine in CH$_2$Cl$_2$[21] gave, after chromatography with heptane as the eluent, bromoiodoferrocene (*S*$_{Fc}$)-**2** in 60% overall yield (based on **4**). The molecular structure of (*S*$_{Fc}$)-**2** could be determined by X-ray diffraction and this confirmed not only its structural integrity but also its *S* absolute configuration (Figure 1, top left; for crystallographic data see the Supporting Information).

The Negishi coupling[22] of (*R*)-**1** and (*S*$_{Fc}$)-**2** worked best when the catalyst system [Pd$_2$(dba)$_3$]·CHCl$_3$/tris(2-furyl)-phosphine (tfp) was used. The desired diastereomer (*R*,*S*$_{Fc}$,*R*$_{Fc}$)-**3**, which has a C$_2$-symmetric biferrocene-2,2″-diyl backbone, was obtained in 78% yield. A small amount of (*R*,*S*$_{Fc}$,*R*$_{Fc}$)-**3** was further reacted with BH$_3$·THF to give the amine−borane complex (*R*,*S*$_{Fc}$,*R*$_{Fc}$)-**3**·BH$_3$. The molecular structure of this compound was determined by X-ray diffraction (Figure 1, top center; for crystallographic data see the Supporting Information).

Diastereomer (*R*,*S*$_{Fc}$,*R*$_{Fc}$)-**3** was further reacted with *n*-BuLi and subsequently quenched with chlorodiphenylphosphine or bis(3,5-dimethyl-4-methyoxyphenyl)chlorophosphine (Scheme 3). In both cases the bromide could be exchanged selectively and the phosphines (*R*,*S*$_{Fc}$,*R*$_{Fc}$)-**6** and (*R*,*S*$_{Fc}$,*R*$_{Fc}$)-**7** were obtained. Oxidation of these two aminophosphines with H$_2$O$_2$ resulted in the formation of phosphine oxides
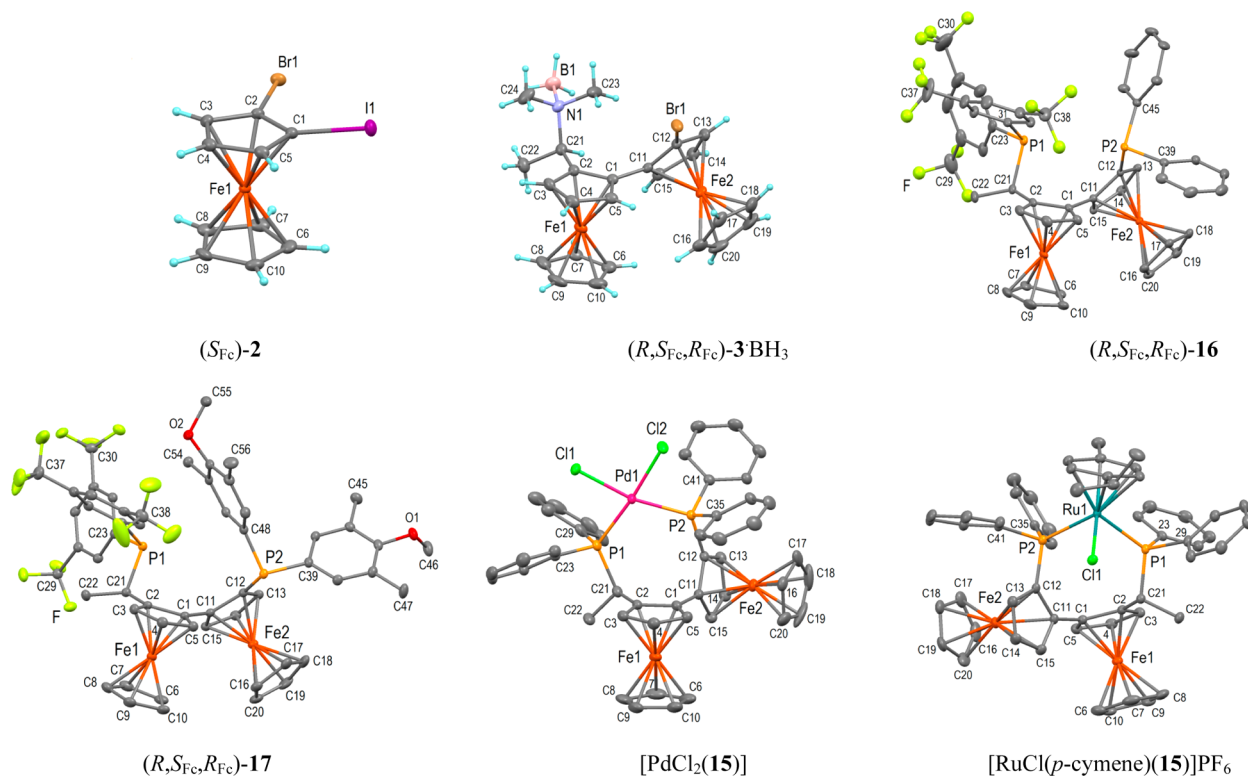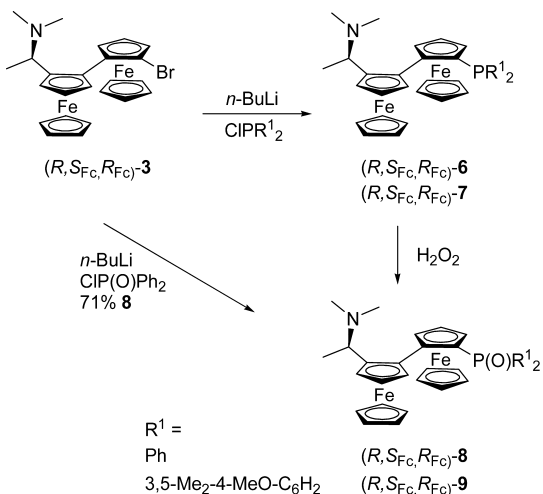
Figure 1. Molecular structures of (S_{Fc})-**2**, (R,S_{Fc},R_{Fc})-**3**·BH₃, (R,S_{Fc},R_{Fc})-**16**, (R,S_{Fc},R_{Fc})-**17**, [PdCl₂(**15**)] (molecule 1), and [RuCl(*p*-cymene)(**15**)]PF₆ showing 50% displacement ellipsoids. Hydrogen atoms and PF₆⁻ are omitted for clarity.

Scheme 3

(R,S_{Fc},R_{Fc})-**8** and (R,S_{Fc},R_{Fc})-**9**. Phosphine oxide (R,S_{Fc},R_{Fc})-**8** could also be obtained directly from **3** when diphenylphosphinyl chloride was used as the electrophile.

In two further steps the dimethylamino group of **8** and **9** was replaced by a dicyclohexyl- or diarylphosphino unit. The reaction of phosphine oxide **8** in acetic acid at 70 °C with dicyclohexylphosphine yielded, after chromatography, the bis phosphine oxide **10b** as the main product. Reaction of **8** with diphenyl- or bis[3,5-bis(trifluoromethyl)phenyl]phosphine mainly gave the phosphine—phosphine oxides **11a** and **12a** (Scheme 4) together with small amounts of bisphosphine oxides **11b** and **12b**.[12a] These mixtures were used in the last step without further separation. In a way similar to that for **8**, compound **9** was reacted with bis[3,5-bis(trifluoromethyl)-

phenyl]phosphine,[19] and the resulting phosphine—phosphine oxide **13a** was isolated in its pure form in 66% yield.

In the last step, the reduction of phosphine oxides **10**—**13** with polymethylhydrosiloxane/titanium isopropoxide[23] gave the desired ligands (R,S_{Fc},R_{Fc})-**14**—**17**. The molecular structures of ligands **16** and **17** were determined by X-ray diffraction and are both shown in Figure 1 (**16**, top right; **17**, bottom left; for crystallographic data see the Supporting Information). It should be mentioned that the substitution patterns of (R,S_{Fc},R_{Fc})-**14**—**17** correspond to those of Walphos ligands SL-W003-1 (**14**), SL-W002-1 (**15**), SL-W001-1 (**16**), and SL-W005-1 (**17**) (Chart 2).

Since we had previously determined the molecular structures of the palladium dichloride complex [PdCl₂(L)][12a,24] and the ruthenium *p*-cymene complex [RuCl(*p*-cymene)(L)]PF₆[25] of Walphos ligand SL-W002-1, the corresponding complexes of the ligand (R,S_{Fc},R_{Fc})-**15** were synthesized. The palladium complex [PdCl₂(**15**)] was obtained by reacting **15** with [PdCl₂(CH₃CN)₂], whereas reaction of the same ligand with the ruthenium dimer [RuCl₂(*p*-cymene)]₂ and subsequent treatment of the reaction mixture with ammonium hexafluorophosphate gave the cationic ruthenium complex [RuCl(*p*-cymene)(**15**)]PF₆. The molecular structures of both complexes of **15** were determined by X-ray diffraction and are depicted in Figure 1 ([PdCl₂(**15**)], bottom center; [RuCl(*p*-cymene)-(**15**)]PF₆, bottom right; for crystallographic data see the Supporting Information).

Structural Features of Ligands and Complexes. The overall structural features of ligands **16** and **17** and of the precursor **3** (Figure 1) are highly comparable. In all three cases the biferrocene backbone adopts a helical arrangement with the mean planes defined by carbons C1—C5 (Cp) and C11—C15 (Cp″), which are rotated with respect to each other by
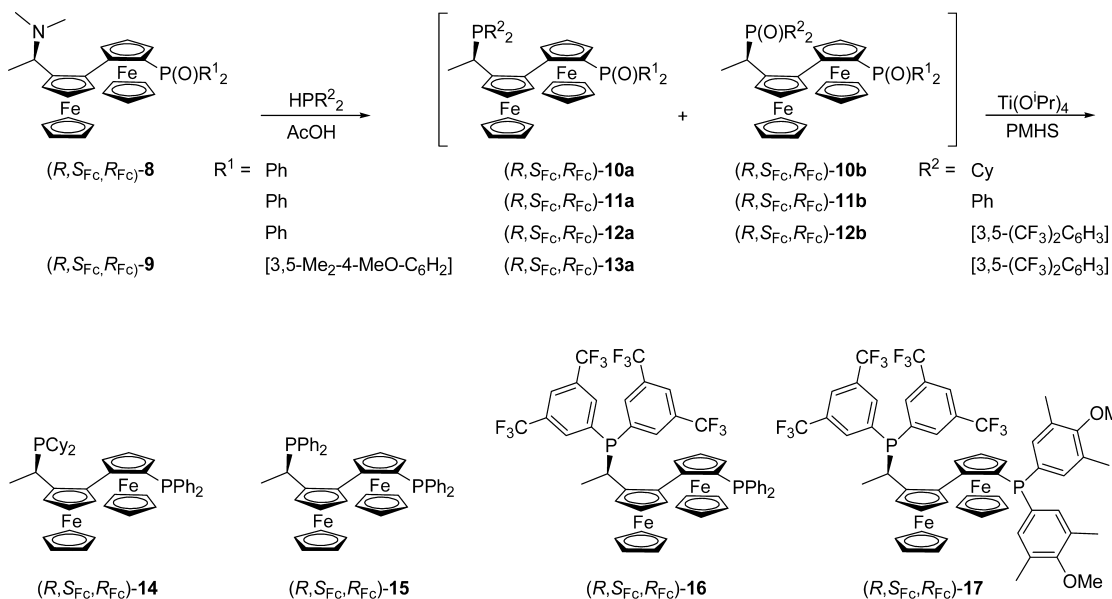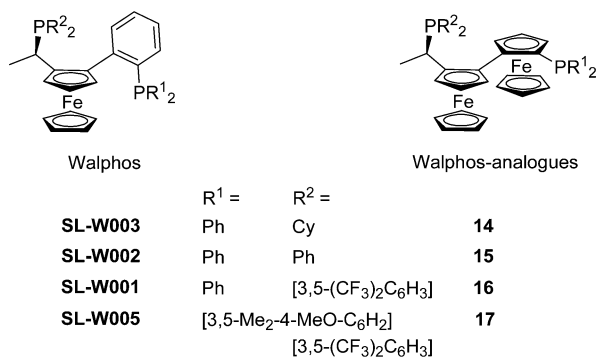
Scheme 4

(R,S_{Fc},R_{Fc})-**8**   R^1 = Ph

(R,S_{Fc},R_{Fc})-**9**   [3,5-Me_2-4-MeO-C_6H_2]

(R,S_{Fc},R_{Fc})-**14**   (R,S_{Fc},R_{Fc})-**15**   (R,S_{Fc},R_{Fc})-**16**   (R,S_{Fc},R_{Fc})-**17**

Chart 2

Walphos   Walphos-analogues

	R^1 =	R^2 =	
SL-W003	Ph	Cy	14
SL-W002	Ph	Ph	15
SL-W001	Ph	[3,5-(CF_3)_2C_6H_3]	16
SL-W005	[3,5-Me_2-4-MeO-C_6H_2]		17
		[3,5-(CF_3)_2C_6H_3]	

preoriented for metal coordination. Complexation of ligand **15** to a PdCl_2 or to a RuCl(p-cymene) unit changes the ligand conformation consistently. The biferrocene backbone of both complexes again adopts a helical arrangement but with a much smaller dihedral angle between Cp and Cp″ than in the free ligand (83.5(1) and 82.3(1)° for the two independent molecules of the palladium complex and 76.9(1)° for the Ru complex). The orientation of the diphenylphosphino units is also adjusted to achieve the complexation of both phosphorus atoms to the metal. This rearrangement places the phenyl rings bound to P2 in comparable positions, as can be seen from the torsion angles C11−C12−P2−C35 and C11−C12−P2−C41 (Pd complex, 62.3(2)/67.6(2) and 177.8(2)/177.8(2)° for the two independent molecules of this crystal structure; Ru complex, 59.7(2) and 167.5(2)°).

124.3(1)° (**16**), 126.0(1)° (**17**) and 123.0(1)° (**3**). The diarylphosphino units of **16** and **17** are reasonably well

As mentioned above, biferrocene ligand **15** can be considered an analogue of Walphos ligand SL-W002-1 (Chart 2), in which
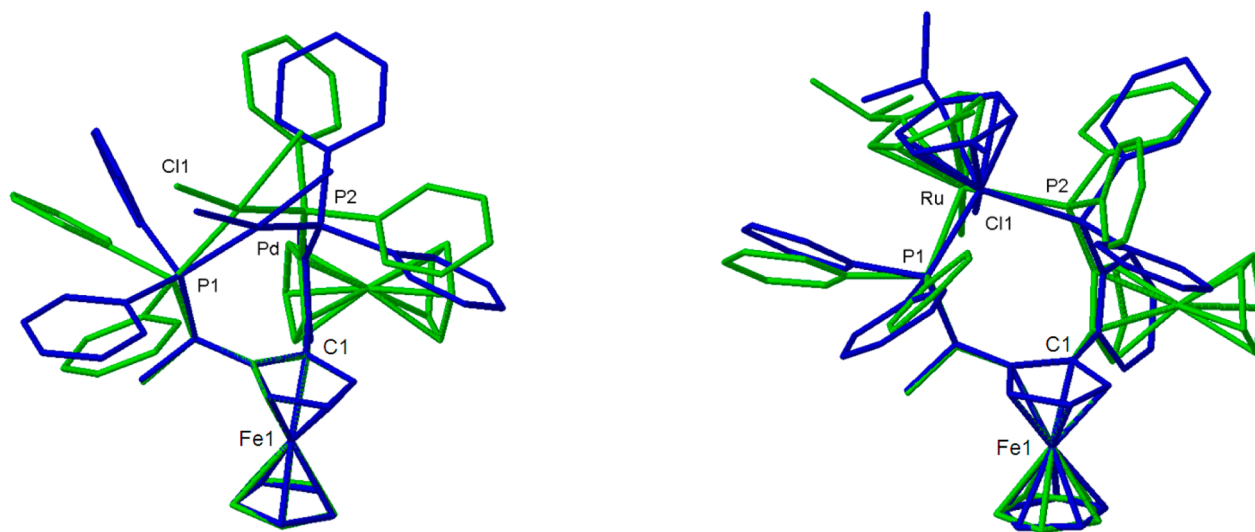
Figure 2. Superpositions of the molecular structures of [PdCl_2(**15**)] and [PdCl_2(SL-W002-1)] (left) and of [RuCl(p-cymene)(**15**)]PF_6 with [RuCl(p-cymene)(SL-W002-1)]PF_6 (right; only the cations of the ruthenium complexes are shown). Ligand **15** is shown in green and SL-W002-1 in blue. In both cases the Cp carbons C1−C5 and Fe1 are superimposed.

Chart 3. Substrates Used for Catalyst Screening
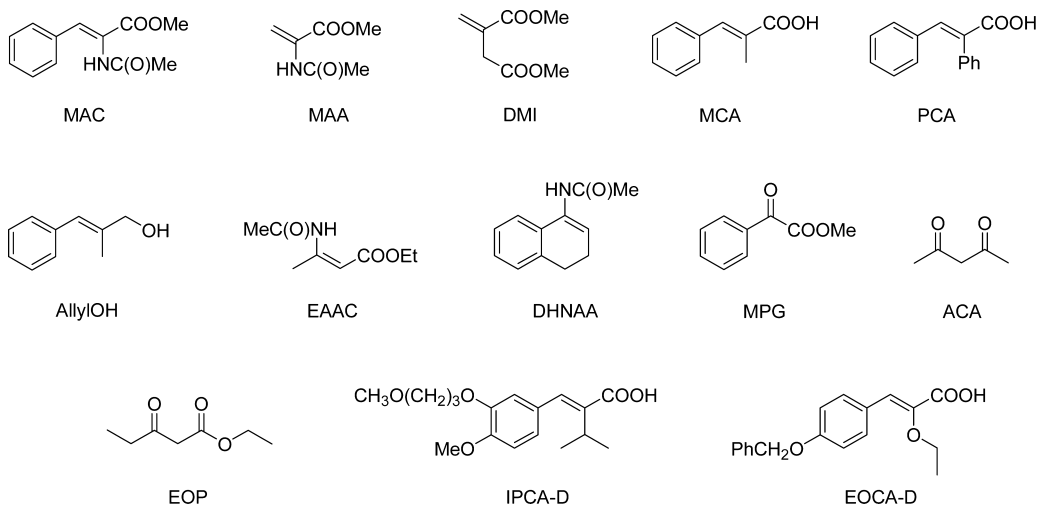
the Walphos backbone phenyl ring is replaced by a second ferrocene unit. It was therefore of interest to see how this change in ligand structure would be reflected in the molecular structures of the corresponding complexes [PdCl$_2$(L)] and [RuCl(*p*-cymene)(L)]PF$_6$ (L = SL-W002-1, **15**). For this purpose geometrical parameters of the corresponding complexes were analyzed (for representative superpositions see Figure 2, and for a comparison of geometrical parameters see the Supporting Information, Table S9).

Superposition of the molecular structures of complexes [PdCl$_2$(**15**)] and [PdCl$_2$(SL-W002-1)] (Figure 2, left) shows that the exchange of the backbone aryl ring of Walphos for a ferrocene unit leads to barely any change in the position of the ethyl side chain carbons and of the side chain bound phosphorus atom (P1; for atom numbering see Figure 1) but it does lead to a significant difference in the position of the phosphorus atom attached to the backbone ferrocene unit (P2). This change follows directly from the geometrical differences of the six-membered aryl unit and the five-membered ferrocene Cp″ ring to which P2 is bound. In comparison to the Walphos complex [PdCl$_2$(SL-W002-1)], P2 in the complex [PdCl$_2$(**15**)] is shifted away from the ferrocene Cp″ ring (P2 is moved away from carbon C1 by about 0.3 Å in the direction of the biferrocene axis). A further significant change is seen in the conformation of the phenyl rings of the two diphenylphosphino units. In particular, one phenyl ring attached to P2 (C35−C40) is rotated in such a way that its interaction with Cp‴ (C16−C20) is minimized. Release of this steric interaction is furthered by an additional out-of-plane deformation that moves P2 a distance of 0.1 Å above Cp″ (C11−C15). This is in contrast to the Walphos complex, in which the corresponding phosphorus atom is also moved out of plane by 0.2 Å but in the opposite direction (below the backbone phenyl ring).

Overall, replacement of the Walphos backbone phenyl ring by a ferrocene unit causes the palladium unit to be positioned higher above and further away from the ferrocene Cp ring. This situation is consistent with a tilt of the square-planar metal unit with Cp (tilt angle of planes Cp/P1−Pd−P2: 78.4(1) and 80.5(1)° in [PdCl$_2$(**15**)] versus 59° in [PdCl$_2$(SL-W002-1)]). In addition, the arrangement of the phenyl rings surrounding the palladium center is changed significantly and the orientational freedom of the phenyl rings at P2 is curtailed. The

slipped π−π interaction between the Cp ring C1−C5 and the phenyl ring C35−C40 (with reference to the atom designation in [PdCl$_2$(**15**)]), which is generally present in PdCl$_2$−Walphos complexes, is absent in [PdCl$_2$(**15**)].

A very similar picture is seen when the molecular structures of the ruthenium complexes [RuCl(*p*-cymene)(**15**)]PF$_6$ and [RuCl(*p*-cymene)(SL-W002-1)]PF$_6$ are superimposed. Replacement of the Walphos ferrocenyl−aryl backbone by a biferrocene unit causes structural changes almost identical with those found for the corresponding palladium complexes. The phosphorus atom P2 and the whole ruthenium cymene unit are moved away from the side chain substituted ferrocene, and this is again reflected in a change of the tilt angle of Cp planes against the P1−Ru−P2 plane (tilt angle 137.7(1)° for the biferrocene complex and 118° for the Walphos complex). The diphenylphosphino phenyl rings are also rearranged, and this change is most pronounced for phenyl ring C35−C40.

In summary, both the PdCl$_2$ and the RuCl(cymene) units coordinate in a fashion very similar to that for Walphos ligand SL-W002-1 and to biferrocene ligand **15**, but it is clear that a change from the Walphos ligand SL-W002-1 to its biferrocene analog (*R*,*S*$_{Fc}$,*R*$_{Fc}$)-**15** results mainly in a conformational change of the phosphine aryl rings, and this leads to a significantly different structural surrounding of the coordinated Pd and Ru metals.

Asymmetric Hydrogenations. All newly synthesized Walphos analogues **14**−**17** of *R*,*S*$_{Fc}$,*R*$_{Fc}$ absolute configuration were tested as ligands in the asymmetric hydrogenation of alkenes and a few ketones (Chart 3). All catalysts were formed in situ by reacting the ligands with an appropriate Rh, Ru, or Ir source, and depending on the substrate, standard test reaction conditions were used. A first set of reactions was carried out on a customized Symyx high-throughput screening (HTS) system with the substrates MAC, MAA, DMI, MCA, AllylOH, (*Z*)-EAAC, DHNAA, and ketone MPG (Chart 3). These reactions were carried out with ligands **14**−**17** in combination with the metal precursors [RhCl(NBD)]$_2$, [Rh(NBD)$_2$]BF$_4$, [Rh(COD)$_2$]O$_3$SCF$_3$, [Ru(COD)(OOCCF$_3$)$_2$], [RuCl$_2$(*p*-cymene)]$_2$, and [Ir(COD)$_2$]BARF (BARF = B[3,5-(CF$_3$)$_2$C$_6$H$_3$]$_4$). For these reactions MeOH or THF was used as the solvent.

The best results were obtained with rhodium catalysts, and these are summarized in Table 1. The ruthenium and iridium

Table 1. Selected High-Throughput Screening Results Obtained with Ligands (R,S_{Fc},R_{Fc})-14−17 in the Rhodium-Catalyzed Hydrogenation of Double Bonds[a]

entry	substrate	metal precursor	ligand	solvent	conversn, %	ee, %
1	MAC	[Rh(NBD)Cl]$_2$	14	THF	>99	47
2	MAC	[Rh(NBD)Cl]$_2$	15	THF	>99	**83**
3	MAC	[Rh(NBD)$_2$]BF$_4$	16	MeOH	>99	**91**
4	MAC	[Rh(NBD)Cl]$_2$	16	THF	18	**81**
5	MAC	[Rh(NBD)$_2$]BF$_4$	17	MeOH	>99	**82**
6	MAA	[Rh(NBD)Cl]$_2$	14	THF	>99	59
7	MAA	[Rh(NBD)$_2$]BF$_4$	15	MeOH	>99	51
8	MAA	[Rh(NBD)$_2$]BF$_4$	16	MeOH	>99	**89**
9	MAA	[Rh(COD)$_2$]O$_3$SCF$_3$	16	THF	>99	**81**
10	MAA	[Rh(NBD)$_2$]BF$_4$	17	MeOH	>99	76
11	DMI	[Rh(NBD)Cl]$_2$	14	THF	99	31
12	DMI	[Rh(NBD)$_2$]BF$_4$	15	MeOH	99	26
13	DMI	[Rh(NBD)$_2$]BF$_4$	16	MeOH	>99	77
14	DMI	[Rh(NBD)Cl]$_2$	17	THF	98	54
15	MCA	[Rh(NBD)Cl]$_2$	14	THF	>99	47
16	MCA	[Rh(NBD)Cl]$_2$	15	THF	80	**94**
17	MCA	[Rh(NBD)$_2$]BF$_4$	16	MeOH	>99	46
18	MCA	[Rh(NBD)$_2$]BF$_4$	17	MeOH	>99	61
19	AllylOH	[Rh(NBD)Cl]$_2$	14	THF	>99	73
20	AllylOH	[Rh(NBD)Cl]$_2$	15	THF	>99	40
21	AllylOH	[Rh(COD)$_2$]O$_3$SCF$_3$	16	THF	>99	**80**
22	AllylOH	[Rh(COD)$_2$]O$_3$SCF$_3$	17	THF	>99	**84**
23	EAAC	[Rh(NBD)Cl]$_2$	14	THF	>99	50
24	EAAC	[Rh(NBD)$_2$]BF$_4$	15	MeOH	>99	40
25	EAAC	[Rh(NBD)Cl]$_2$	16	THF	60	42
26	EAAC	[Rh(NBD)Cl]$_2$	17	THF	86	49
27	DHNAA	[Rh(NBD)Cl]$_2$	14	THF	>99	19
28	DHNAA	[Rh(NBD)Cl]$_2$	15	THF	81	24
29	DHNAA	[Rh(NBD)Cl]$_2$	16	THF	16	28
30	DHNAA	[Rh(NBD)$_2$]BF$_4$	17	MeOH	>99	22
31	MPG	[Rh(COD)$_2$]O$_3$SCF$_3$	14	THF	99	51
32	MPG	[Rh(NBD)Cl]$_2$	15	THF	99	46
33	MPG	[Rh(NBD)Cl]$_2$	16	THF	>99	50
34	MPG	[Rh(NBD)Cl]$_2$	17	THF	99	44

[a]Reaction conditions: substrate, 41.67 μmol; catalyst, 1.67 μmol; catalyst loading S/C, 25; V_{total}, 500 μL.

precursors tested gave only poor to moderate results (see the Supporting Information, Table S1). Conversions and product enantiomeric excesses of ≥80% could be reached in the rhodium-catalyzed hydrogenations for methyl acetamidoacrylate (MAA), α-substituted cinnamic acid derivatives such as methyl (Z)-α-acetamidocinnamate (MAC) and (E)-2-methylcinnamic acid (MCA), and (E)-2-methyl-3-phenyl-prop-2-enol (AllylOH). The best results for the hydrogenation of substrates MAC, MAA, and DMI were obtained with ligands 15 and 16 in combination with the precursor [Rh(NBD)$_2$]BF$_4$ in MeOH (Table 1, entries 2−4, 8, 9, and 13) and for MCA with [RhCl(NBD)]$_2$ in THF (Table 1, entry 16). In the case of AllylOH the combination of ligands 16 or 17 together with precursor [Rh(COD)$_2$]O$_3$SCF$_3$ in THF performed the best (Table 1, entries 21 and 22).

For some of the substrates (MAC, DMI, MCA) the results obtained with ligands 15 and 16 compare reasonably well with data reported for the corresponding Walphos ligands SL-W002 and SL-W001.

As a result, it seemed interesting to investigate the performance of these ligands in more detail and to extend the scope of substrates to (E)-2-phenylcinnamic acid (PCA) and to the commercially interesting cinnamic acid derivatives

IPCA-D[12b,13g,26] and EOCA-D[13k,27] (Chart 3), as well as to the ketones acetylacetone (ACA) and ethyl 3-oxo-pentanoate (EOP). Hydrogenations were carried out with the substrates MAC, MAA, DMI, MAC, PCA, IPCA-D, EOCA-D, ACA, and EOP (Chart 3), with biferrocene ligands (R,S_{Fc},R_{Fc})-15 and (R,S_{Fc},R_{Fc})-16, with Walphos ligands SL-W001-1 (with R,R_{Fc} configuration) and SL-W002-2 (with the opposite S,S_{Fc} configuration), and with precursors [Rh(NBD)$_2$]BF$_4$ in MeOH or [RhCl(NBD)]$_2$ in THF. The results of these hydrogenations are given in Table 2. The majority of reactions were carried out in single experiments in either a glass or a steel autoclave. For biferrocene ligands 15 and 16 and substrates MAC, MAA, DMI, and, in part, MCA not all the high-throughput screening results were repeated (Table 2, entries 1−8), but in these cases at least one reaction for each substrate was run in a single experiment.

For example, the hydrogenation of MAA was carried out with ligand 15, precursor [Rh(NBD)$_2$]BF$_4$ in MeOH, and an S/C ratio of 100. The product was obtained with 100% conversion and 50% ee, and this compares very well with the HTS result (100% conversion and 51% ee; Table 2, entry 3).

Comparison of the data shows that substrates MAC, MAA, and DMI can be hydrogenated to products with good to

Table 2. Comparison of Hydrogenation Data Obtained with Use of Walphos and Biferrocene Ligands

entry	substrate	precursor	solvent	T, °C	p, atm	Walphos ligand	S/C	conversn, %	ee, %	BiFc ligand	S/C	conversn, %	ee, %
1	MAC	[Rh(NBD)$_2$]BF$_4$	MeOH	20	1	W002-2	100	100	**88**	15	25	100	21^a
2	MAC	[Rh(NBD)$_2$]BF$_4$	MeOH	20	1	W001-1	100	100	63	16	25	100	**91**^{a}
3	MAA	[Rh(NBD)$_2$]BF$_4$	MeOH	20	1	W002-2	100	100	96	15	25	100	51^a
4	MAA	[Rh(NBD)$_2$]BF$_4$	MeOH	20	1	W001-1	100	100	**97**	16	25	100	89^a
5	DMI	[Rh(NBD)$_2$]BF$_4$	MeOH	20	1	W002-2	100	100	87	15	25	99	26^a
6	DMI	[Rh(NBD)$_2$]BF$_4$	MeOH	20	1	W001-1	100	100	52	16	25	100	77^a
7	MCA	[Rh(NBD)$_2$]BF$_4$	MeOH	20	20	W002-2	100	99	62	15	25	100	40^a
8	MCA	[Rh(NBD)$_2$]BF$_4$	MeOH	20	20	W001-1	100	100	**83**	16	25	100	46^a
9	MCA	[RhCl(NBD)]$_2$	THF	20	20	W002-2	100	11	n.d.	15	100	19	76
10	MCA	[RhCl(NBD)]$_2$	THF	20	20	W002-2	25	14	n.d.	15	25	63	**80**
11	PCA	[Rh(NBD)$_2$]BF$_4$	MeOH	20	50	W002-2	100	77	**89**	15	100	100	29
12	PCA	[Rh(NBD)$_2$]BF$_4$	MeOH	20	50	W001-1	100	100	82	16	100	100	44
13	IPCA-D	[Rh(NBD)$_2$]BF$_4$	MeOH	20	50	W002-2	100	100	74	15	25	100	34
14	IPCA-D	[Rh(NBD)$_2$]BF$_4$	MeOH	20	50	W001-1	100	100	**94**	16	25	100	54
15	IPCA-D	[RhCl(NBD)]$_2$	THF	20	50	W002-2	25	7	n.d.	15	25	21	**87**
16	EOCA-D^b	[Rh(NBD)$_2$]BF$_4$	MeOH	20	3.5	W002-2	25	100	80	15	25	100	19
17	EOCA-D^b	[Rh(NBD)$_2$]BF$_4$	MeOH	20	3.5	W001-1	40	80	**87**	16	25	100	44
18	EOCA-D^b	[RhCl(NBD)]$_2$	THF	20	20	W002-2	25	100	86	15	25	100	16
19	ACA^c	[RuI$_2$(p-cymene)]$_2$	MeOH	80	80	W002-2	500	100	85	15	500	100	80
20	ACA^c	[RuI$_2$(p-cymene)]$_2$	MeOH	80	80	W001-1	500	100	**96**	16	500	100	**85**
21	EOP^c	[RuI$_2$(p-cymene)]$_2$	EtOH	80	80	W002-2	100	100	76	15	100	100	94
22	EOP^c	[RuI$_2$(p-cymene)]$_2$	EtOH	80	80	W001-1	100	100	**93**	16	100	100	75

^{a}HTS results. ^{b}Additive NaOMe. ^{c}Additive HCl.

excellent ee values (77−97%; Table 2, entries 1−6) on using either the Walphos ligands or their biferrocene analogues. However, analogous ligands do not perform equally well. For example, the hydrogenation of MAC with the Walphos ligand SL-W002 led to the product with 88% ee, while that with the analogous ligand **15** gave rise to only 21% ee. The Walphos ligand SL-W001 gave 63% ee, while its biferrocene analogue **16** gave the product with 91% ee (Table 2, entries 1 and 2).

On the basis of the HTS results, for the hydrogenation of MCA the catalyst system **15**/[RhCl(NBD)]$_2$/THF seemed to be an interesting alternative to the original SL-W001/[Rh(NBD)$_2$]BF$_4$/MeOH system (Table 1, entry 16). However, a number of single experiments showed that, in order to achieve useful conversions, not only high pressure but also a high catalyst load is required. In an effort to identify the appropriate reaction conditions, a number of test runs were carried out. A conversion of 15% was obtained with 1% of catalyst and a hydrogen pressure of 5 bar, but an increase in the pressure to 50 bar only led to a marginal improvement in yield to 17%. Only when the catalyst load was raised to 4% did the conversion increase significantly. At a pressure of 20 bar 63% (Table 2, entry 10) and at 50 bar 90% conversion was reached.

Interestingly, when ligand **15** was replaced by Walphos SL-W002 and the catalyst system SL-W002/[RhCl(NBD)]$_2$/THF was applied, conversion became very low even when 4% of catalyst was used (Table 2, entries 9 and 10). On the basis of the high catalyst load required, it is clear that the **15**/[RhCl(NBD)]$_2$/THF system must be considered of little practical use, despite the reasonably high product ee obtained (80%; Table 2, entry 10).

Like MCA, substrates PCA, IPCA-D, and EOCA-D represent 2-substituted cinnamic acid derivatives with the carboxyl group in a position *trans* to the aryl ring at position 3. In all of these cases the [Rh(NBD)$_2$]BF$_4$/MeOH system performed much better with Walphos ligands than with their analogous

biferrocene ligands (PCA, SL-W002/**15**, 89/29% ee; IPCA-D, SL-W001/**16**, 94/54% ee; EOCA-D, SL-W001/**16**, 87/44% ee; Table 2, entries 11, 14, and 17).

In a way similar to that for MCA, the substrate IPCA-D gave the **15**/[RhCl(NBD)]$_2$/THF catalyst system product with a reasonably high ee value (87%)—albeit again with very low conversion (Table 2, entry 15).

Diketone ACA and β-keto ester EOP were hydrogenated at 80 bar and 80 °C in MeOH (ACA) or EtOH (EOP) with [RuI$_2$(p-cymene)]$_2$ as the metal precursor. The best results were obtained with Walphos ligand SL-W001 (ACA 96% ee and EOP 93% ee, quantitative conversion), but with these substrates the biferrocene analogue **16** also performed well (ACA 85% ee and EOP 75% ee, quantitative conversion; Table 2, entries 21 and 22).

In all reactions the absolute configurations of products were determined, and these are given in Table 3. It is important to note that in the hydrogenation reactions we used Walphos ligands with different absolute configurations. Ligand SL-W001-1 had an R,R_{Fc} configuration, and ligand SL-W002-2 had an S,S_{Fc} configuration. For ease of comparison the results given in Table 3 are normalized. Results are given for ligands with the R configuration at the ferrocene side chain carbon (Walphos ligands with R,R_{Fc} and biferrocene ligands with R,S_{Fc},R_{Fc} configuration).

From the results in Table 3 it is immediately apparent that the product absolute configurations obtained with analogous Walphos[28] and biferrocene ligands are not identical. For example, with the substrate MAC and ligands SL-W001-1 and SL-W002-1 (both with the R,R_{Fc} configuration) the product with the S configuration was formed. However, with biferrocenes (R,S_{Fc},R_{Fc})-**15** and (R,S_{Fc},R_{Fc})-**16** products of S and R configurations, respectively, were obtained (Table 3, entries 1 and 2). It is also clear that for all alkenes tested the use of Walphos ligands SL-W001 and SL-W002 led to products of

Table 3. Product Absolute Configurations Given for Walphos Ligands of R,R_{Fc} and Biferrocene Ligands of R,S_{Fc},R_{Fc} Absolute Configuration

entry	substrate	precursor	Walphos ligand	abs config'n	BiFc ligand	abs config'n
1	MAC	$[Rh(NBD)_2]BF_4$	W002	S	15	S
2	MAC	$[Rh(NBD)_2]BF_4$	W001	S	16	R
3	MAA	$[Rh(NBD)_2]BF_4$	W002	S	15	S
4	MAA	$[Rh(NBD)_2]BF_4$	W001	S	16	R
5	DMI	$[Rh(NBD)_2]BF_4$	W002	R	15	R
6	DMI	$[Rh(NBD)_2]BF_4$	W001	R	16	S
7	MCA	$[Rh(NBD)_2]BF_4$	W002	S	15	R
8	MCA	$[Rh(NBD)_2]BF_4$	W001	S	16	S
9	MCA	$[RhCl(NBD)]_2$	W002		15	R
10	MCA	$[RhCl(NBD)]_2$	W002		15	R
11	PCA	$[Rh(NBD)_2]BF_4$	W002	R	15	R
12	PCA	$[Rh(NBD)_2]BF_4$	W001	R	16	R
13	IPCA-D	$[Rh(NBD)_2]BF_4$	W002	R	15	R
14	IPCA-D	$[Rh(NBD)_2]BF_4$	W001	R	16	R
15	IPCA-D	$[RhCl(NBD)]_2$	W002		15	S
16	EOCA-D	$[Rh(NBD)_2]BF_4$	W002	S	15	S
17	EOCA-D	$[Rh(NBD)_2]BF_4$	W001	S	16	S
18	EOCA-D	$[RhCl(NBD)]_2$	W002		15	S
19	ACA	$[RuI_2(p\text{-}cymene)]_2$	W002	R,R	15	S,S
20	ACA	$[RuI_2(p\text{-}cymene)]_2$	W001	S,S	16	S,S
21	EOP	$[RuI_2(p\text{-}cymene)]_2$	W002	S	15	S
22	EOP	$[RuI_2(p\text{-}cymene)]_2$	W001	S	16	S

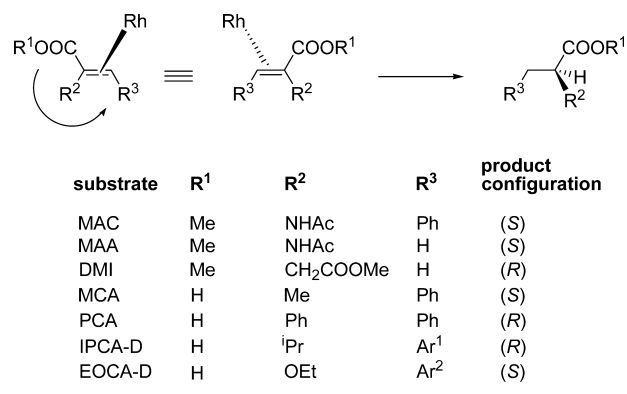identical configuration (MAC, MAA, MCA, EOCA-D, S; DMI, PCA, IPCA-D, R), but this is not the case for the biferrocene ligands 15 and 16.

A closer analysis of the product absolute configurations obtained with Walphos ligands showed another surprising feature. It is evident that in order to obtain a product of S configuration, in the enantiomer-determining step of the hydrogenation reaction the substrate must be coordinated to the metal through its Si side. A structural analysis showed that in order to account for the observed product absolute configurations, all alkene substrates used must coordinate to the metal in a uniform way. In the enantiomer-determining step rhodium has to coordinate to the side of the alkene that has the carboxyl (or alkoxycarbonyl) group (COOR^1), with the α (R^2) and the β substituent (R^3) arranged in a counterclockwise manner (Chart 4). This order does not depend on whether or not the substituent R^2 is able to coordinate to the metal. Such a compelling relationship was not observed for the hydrogenation of ketones or for any reactions in which the biferrocene ligands were used.

CONCLUSION

Four biferrocene analogues of Walphos ligands were prepared by replacing the Walphos ferrocenyl–aryl backbone with a biferrocene unit. The biferrocene backbone was built up by a Negishi coupling of two nonracemic ferrocene fragments. For this purpose a synthesis had to be developed for (S)-2-bromoiodoferrocene. The newly synthesized ligands were tested in both a high-throughput screening system and single experiments in the hydrogenation of alkenes and ketones. Moderate to high product ee values were obtained for acrylic

Chart 4

substrate	R^1	R^2	R^3	product configuration
MAC	Me	NHAc	Ph	(S)
MAA	Me	NHAc	H	(S)
DMI	Me	CH_2COOMe	H	(R)
MCA	H	Me	Ph	(S)
PCA	H	Ph	Ph	(R)
IPCA-D	H	^iPr	Ar^1	(R)
EOCA-D	H	OEt	Ar^2	(S)

and cinnamic acid derivatives as well as for two ketones. A comparative study was also carried out with two biferrocene-based ligands (15 and 16) and their analogous Walphos ligands (SL-W002 and SL-W001).

A comparison of the structural features of the complexes $[PdCl_2(15)]$ and $[RuCl(p\text{-}cymene)(15)]PF_6$ with those of $[PdCl_2(SL\text{-}W002)]$ and $[RuCl(p\text{-}cymene)(SL\text{-}W002)]PF_6$ showed that the replacement of the Walphos backbone aryl ring by a ferrocene unit results mainly in a change in the position of the diphenylphosphino unit directly attached to the biferrocene backbone. This leads to a conformational change of the phosphine aryl rings and thus to a significantly different structural surrounding of the coordinated Pd and Ru metals.

The Walphos ligands and their analogous biferrocene ligands showed significantly different performances in the hydrogenation reactions. These reactions gave not only different product ee values but, even more significantly, for a number of substrates products with opposite absolute configurations were obtained. Overall, only in some cases did the biferrocene-based ligands perform as well or nearly as well as their Walphos analogues.

Interestingly, in the rhodium-catalyzed hydrogenations with Walphos ligands SL-W001 and SL-W002 it was found that, in order to account for the observed product absolute configurations, all alkene substrates used must coordinate in the enantioselective step to the metal in a uniform way. This structural correlation does not hold for the corresponding biferrocene ligands 15 and 16.

ASSOCIATED CONTENT

Ⓢ Supporting Information

Text, figures, tables, and CIF files giving full experimental descriptions and spectroscopic data for all newly synthesized ligands and complexes as well as detailed hydrogenation and transfer hydrogenation data, crystallographic and geometric data for precursors (S_{Fc})-2 and (R,S_{Fc},R_{Fc})-3·BH$_3$, ligands (R,S_{Fc},R_{Fc})-16 and (R,S_{Fc},R_{Fc})-17, and complexes $[PdCl_2(15)]$ and $[RuCl(p\text{-}cymene)(15)]PF_6$. This material is available free of charge via the Internet at http://pubs.acs.org.

AUTHOR INFORMATION

Corresponding Author
*E-mail: walter.weissensteiner@univie.ac.at.

Notes

The authors declare no competing financial interest.

■ REFERENCES

(1) (a) Ohkuma, T.; Kurono, K. In *Privileged chiral ligands and catalysts*; Zhou, Q.-L., Ed.; Wiley-VCH: Weinheim, Germany, 2011; pp 1−53. (b) *Asymmetric catalysis on industrial scale*; Blaser, H.-U.; Federsel, H.-J., Eds.; Wiley-VCH: Weinheim, Germany, 2011. (c) *Catalytic Asymmetric Synthesis*; Ojima, I., Ed.; Wiley: New York, 2000. (d) Noyori, R. *Asymmetric Catalysis in Organic Synthesis*; Wiley: New York, 1994.

(2) Miyashita, A.; Yasuda, A.; Takaya, H.; Toriumi, K.; Ito, T.; Souchi, T.; Noyori, R. *J. Am. Chem. Soc.* **1980**, *102*, 7932−7934. (b) Miyashita, A.; Takaya, H.; Souchi, T.; Noyori, R. *Tetrahedron* **1984**, *40*, 1245−1253.

(3) (a) Lam, F. L.; Kwong, F. Y.; Chan, A. S. C. In *Organometallic Chemistry*; Shengming, M., Ed.; Springer: Berlin, 2011; Vol. *36*, pp 29−66. (b) Arshad, N.; Kappe, C. O. *Adv. Heterocycl. Chem.* **2010**, *99*, 33−59. (c) Shimizu, H.; Nagasaki, I.; Sayo, N.; Saito, T. In *Phosphorus Ligands in Asymmetric Catalysis*; Börner, A., Ed.; Wiley-VCH: Weinheim, Germany, 2008; Vol. *1*, pp 207−260. (d) Li, Y.-M.; Kwong, F.-Y.; Yu, W.-Y.; Chan, A. S. C. *Coord. Chem. Rev.* **2007**, *251*, 2119−2144. (e) Shimizu, H.; Nagasaki, I.; Saito, T. *Tetrahedron* **2005**, *61*, 5405−5432.

(4) Sawamura, M.; Yamauchi, A.; Takegawa, T.; Ito, Y. *Chem. Commun.* **1991**, 874−875.

(5) (a) Kuwano, R.; Uemura, T.; Saitoh, M.; Ito, Y. *Tetrahedron: Asymmetry* **2004**, *15*, 2263−2271. (b) Kuwano, R.; Sawamura, M.; Okuda, S.; Asai, T.; Ito, Y.; Redon, M.; Krief, A. *Bull. Chem. Soc. Jpn.* **1997**, *70*, 2807−2282. (c) Sawamura, M.; Hamashima, H.; Sugawa, M.; Kuwano, R.; Ito, Y. *Organometallics* **1995**, *14*, 4549. (d) Sawamura, M.; Hamashima, H.; Ito, Y. *Tetrahedron: Asymmetry* **1991**, *2*, 593−569.

(6) (a) Nettekoven, U.; Widhalm, M.; Kamer, P. C. J.; van Leeuwen, P. W. N. M.; Mereiter, K.; Lutz, M.; Spek, A. L. *Organometallics* **2000**, *19*, 2299−2309. (b) Nettekoven, U.; Widhalm, M.; Kalchhauser, H.; Kamer, P. C. J.; van Leeuwen, P. W. N. M.; Lutz, M.; Spek, A. L. *J. Org. Chem.* **2001**, *66*, 759−770.

(7) (a) Xiao, L.; Mereiter, K.; Spindler, F.; Weissensteiner, W. *Tetrahedron: Asymmetry* **2001**, *12*, 1105−1108. (b) Espino, G.; Xiao, L.; Puchberger, M.; Mereiter, K.; Spindler, F.; Manzano, B. R.; Jalon, F. A.; Weissensteiner, W. *Dalton Trans.* **2009**, 2751−2763.

(8) Kuwano, R. In *Chiral Ferrocenes in Asymmetric Catalysis*; Dai, L.-X., Hou, X.-L., Eds.; Wiley-VCH: Weinheim, Germany, 2010; pp 283−305.

(9) Lotz, M.; Kramer, G.; Knochel, P. *Chem. Commun.* **2002**, 2546−2547.

(10) Schuecker, R.; Mereiter, K.; Spindler, F.; Weissensteiner, W. *Adv. Synth. Catal.* **2010**, *352*, 1063−1074.

(11) (a) *Asymmetric Catalysis*; Dai, L.-X., Hou, X.-L., Eds.; Wiley-VCH: Weinheim, Germany, 2010. (b) Manoury, E.; Poli, R. In *Catalysis by Metal Complexes*; Peruzzini, M., Gonsalvi, L., Eds.; Springer: Berlin, 2011; Vol. *37*, pp 121−149. (c) *Ferrocenes: Ligands, Materials and Biomolecules*; Stepnicka, P., Ed.; Wiley: Weinheim, Germany, 2008. (d) Gomez Arrayás, R.; Adrio, J.; Carretero, J. C. *Angew. Chem., Int. Ed.* **2006**, *45*, 7674−7715. (e) Barbaro, P.; Bianchini, C.; Giambastiani, G.; Parisel, S. L. *Coord. Chem. Rev.* **2004**, *248*, 2131−2150. (f) Atkinson, R. C. J.; Gibson, V. C.; Long, N. J. *Chem. Soc. Rev.* **2004**, *33*, 313−328.

(12) (a) Wang, Y.; Sturm, T.; Steurer, M.; Arion, V. B.; Mereiter, K.; Spindler, F.; Weissensteiner, W. *Organometallics* **2008**, *27*, 1119−1127. (b) Sturm, T.; Weissensteiner, W.; Spindler, F. *Adv. Synth. Catal.* **2003**, *345*, 160−164.

(13) (a) Stewart, G. W.; Shevlin, M.; Yamagata, A. D. G.; Gibson, A. W.; Keen, S. P.; Scott, J. P. *Org. Lett.* **2012**, *14*, 5440−5443. (b) Duan, Z.-C.; Wang, L.-Z.; Song, X.-J.; Hu, X.-P; Zheng, Z. *Tetrahedron: Asymmetry* **2012**, *23*, 508−514. (c) Yu, C.-B.; Gao, K.; Wang, D.-S.; Shi, L.; Zhou, Y.-G. *Chem. Commun.* **2011**, 5052−5054. (d) Maj, A. M.; Suisse, I.; Meliet, C.; Agbossou-Niedercorn, F. *Tetrahedron: Asymmetry* **2010**, *21*, 2010−2014. (e) Alimardanov, A.; Nikitenko, A.; Connolly, T. J.; Feigelson, G.; Chan, A. W.; Ding, Z.; Ghosh, M.; Shi, X.; Ren, J.; Hansen, E.; Farr, R.; MacEwan, M.; Tadayon, S.; Springer, D. M.; Kreft, A. F.; Ho, D. M.; Potoski, J. R. *Org. Process Res. Dev.* **2009**, *13*, 1161−1168. (f) Krska, S. W.; Mitten, J. V.; Dormer, P. G.; Mowrey, D.; Machrouhi, F.; Sun, Y.; Nelson, T. D. *Tetrahedron* **2009**, *65*, 8987−8994. (g) Andrushko, N.; Andrushko, V.; Thyrann, T.; König, G.; Börner, A. *Tetrahedron Lett.* **2008**, *49*, 5980−5982. (h) Herold, P.; Stutz, S.; Mah, R.; Stojanovic, A.; Lyothier, I.; Behnke, D.; Spindler, F.; Bappert, E. PCT Int. Appl. WO 2007085651, 2007. (i) Moran, W. J.; Morken, J. P. *Org. Lett.* **2006**, *8*, 2413−2415. (j) Stephenson, P.; Kondor, B.; Licence, P.; Scovell, K.; Ross, S. K.; Poliakoff, M. *Adv. Synth. Catal.* **2006**, *348*, 1605−1610. (k) Houpis, I. N.; Patterson, L. E.; Alt, C. A.; Rizzo, J. R.; Zhang, T. Y.; Haurez, M. *Org. Lett.* **2005**, *7*, 1947−1950. (l) Pugin, B.; Studer, M.; Kuesters, E.; Sedelmeier, G.; Feng, X. *Adv. Synth. Catal.* **2004**, *346*, 1481−1486. (m) Morgan, J. B.; Morken, J. P. *J. Am. Chem. Soc.* **2004**, *126*, 15338−15339. (n) Bänziger, M.; Cercus, J.; Hirt, H.; Laumen, K.; Malan, C.; Spindler, F.; Struber, F.; Troxler, T. *Tetrahedron: Asymmetry* **2003**, *14*, 3469−3477.

(14) Moberg, V.; Haukka, M.; Koshevoy, I. O.; Ortiz, R.; Nordlander, E. *Organometallics* **2007**, *26*, 4090−4093.

(15) (a) Li, Q.; Ding, C.-H.; Li, X.-H.; Weissensteiner, W.; Hou, X.-L. *Synthesis* **2012**, *44*, 265−271. (b) Chatterjee, I.; Fröhlich, R.; Studer, A. *Angew. Chem., Int. Ed.* **2011**, *50*, 11257−11260. (c) Chou, C.-M.; Chatterjee, I.; Studer, A. *Angew. Chem., Int. Ed.* **2011**, *50*, 8614−8617. (d) Ishida, K.; Kusama, H.; Iwasawa, N. *J. Am. Chem. Soc.* **2010**, *132*, 8842−8843. (e) Hojo, D.; Noguchi, K.; Tanaka, K. *Angew. Chem., Int. Ed.* **2009**, *48*, 8129−8132. (f) Jana, C. K.; Grimme, S.; Studer, A. *Chem. Eur. J.* **2009**, *15*, 9078−9084. (g) Hojo, D.; Noguchi, K.; Hirano, M.; Tanaka, K. *Angew. Chem., Int. Ed.* **2008**, *47*, 5820−5822. (h) Jana, C. K.; Studer, A. *Chem. Eur. J.* **2008**, *14*, 6326−6328. (i) Chen, I.-H.; Oisaki, K.; Kanai, M.; Shibasaki, M. *Org. Lett.* **2008**, *10*, 5151−5154. (j) Jana, C. K.; Studer, A. *Angew. Chem., Int. Ed.* **2007**, *46*, 6542−6544. (k) Tanaka, K.; Hagiwara, Y.; Hirano, M. *Eur. J. Org. Chem.* **2006**, 3582−3595. (l) Tanaka, K.; Hagiwara, Y.; Noguchi, K. *Angew. Chem., Int. Ed.* **2005**, *44*, 7260−7263.

(16) (a) Komanduri, V.; Krische, M. J. *J. Am. Chem. Soc.* **2006**, *128*, 16448−16449. (b) Kong, J.-R.; Ngai, M.-Y.; Krische, M. J. *J. Am. Chem. Soc.* **2006**, *128*, 718−719. (c) Kreis, M.; Friedmann, C. J.; Bräse, S. *Chem. Eur. J.* **2005**, *11*, 7387−7394.

(17) (a) Voigtritter, K. R.; Isley, N. A.; Moser, R.; Aue, D. H.; Lipshutz, B. H. *Tetrahedron* **2012**, *68*, 3410−3416. (b) Lipshutz, B. H.; Frieman, B. A.; Unger, J. B.; Nihan, D. M. *Can. J. Chem.* **2005**, *83*, 606−614. (c) Lipshutz, B. H.; Noson, K.; Chrisman, W.; Lower, A. *J. Am. Chem. Soc.* **2003**, *125*, 8779−8789. (d) Lipshutz, B. H.; Servesko, J. M. *Angew. Chem., Int. Ed.* **2003**, *42*, 4789−4792.

(18) (a) Sole, C.; Gulyas, H.; Fernandez, E. *Chem. Commun.* **2012**, *48*, 3769−3771. (b) Wisniewska, H. M.; Jarvo, E. R. *Chem. Sci.* **2011**, *2*, 807−810. (c) Marinho, V. R.; Burke, A. J. *Synth. Commun.* **2009**, *39*, 4423−4428. (d) Feng, X.; Yun, J. *Chem. Commun.* **2009**, 6577−6579. (e) Panteleev, J.; Menard, F.; Lautens, M. *Adv. Synth. Catal.* **2008**, *350*, 2893−2902. (f) Schäffner, B.; Holz, J.; Verevkin, S. P.; Börner, A. *ChemSusChem* **2008**, *1*, 249−253. (g) Stemmler, R. T.; Bolm, C. *Adv. Synth. Catal.* **2007**, *349*, 1185−1198. (h) Umeda, R.; Studer, A. *Org. Lett.* **2007**, *9*, 2175−2178. (i) Chuzel, O.; Deschamp, J.; Chausteur, C.; Riant, O. *Org. Lett.* **2006**, *8*, 5943−5946. (j) Godard, C.; Ruiz, A.; Claver, C. *Helv. Chim. Acta* **2006**, *89*, 1610−1622. (k) Axtell, A. T.; Klosin, J.; Abboud, K. A. *Organometallics* **2006**, *25*, 5003−5009. (l) Cho, C.-W.; Krische, M. J. *Org. Lett.* **2006**, *8*, 3873−3876. (m) Llamas, T.; Arrayás, R. G.; Carretero, J. C. *Org. Lett.* **2006**, *8*, 1795−1798. (n) Phua, P. H.; White, A. J. P.; deVries, J. G.; Hii, K. K. *Adv. Synth. Catal.* **2006**, *348*, 587−592. (o) Deschamp, J.; Chuzel, O.;

Hannedouche, J.; Riant, O. *Angew. Chem., Int. Ed.* **2006**, *45*, 1292–1297. (p) Lipshutz, B. H.; Frieman, B. A.; Unger, J. B.; Nihan, D. M. *Can. J. Chem.* **2005**, *83*, 606–614. (q) Munoz, M. P.; Adrio, J.; Carretero, J. C.; Echavarren, A. M. *Organometallics* **2005**, *24*, 1293–1300. (r) Berkowitz, D. B.; Maiti, G. *Org. Lett.* **2004**, *6*, 2661–2664. (s) Markert, C.; Pfaltz, A. *Angew. Chem., Int. Ed.* **2004**, *43*, 2498–2500.

(19) For an alternative approach see: Groß, M. A.; Mereiter, K.; Wang, Y.; Weissensteiner, W. *J. Organomet. Chem.* **2012**, *716*, 32–38.

(20) (a) Riant, O.; Argouarch, G.; Guillaneux, D.; Samuel, O.; Kagan, H. B. *J. Org. Chem.* **1998**, *63*, 3511–3514. (b) Rebiere, F.; Riant, O.; Ricard, L.; Kagan, H. B. *Angew. Chem., Int. Ed. Engl.* **1993**, *32*, 568–70.

(21) Fan, C.-A.; Ferber, B.; Kagan, H. B.; Lafon, O.; Lesot, P. *Tetrahedron: Asymmetry* **2008**, *19*, 2666–2677.

(22) (a) Negishi, E.-I.; Hu, Q.; Huang, Z.; Qian, M.; Wang, G. *Aldrichim. Acta* **2005**, *38*, 71–88. (b) Negishi, E.-I.; Zeng, X.; Tan, Z.; Qian, M.; Hu, Q.; Huang, Z. In *Metal-Catalyzed Cross-Coupling Reactions*; De Meijere, A., Diederich, F., Eds.; Wiley-VCH: Weinheim, Germany, 2004; Vol. 2, pp 815–889.

(23) Coumbe, T.; Lawrence, N. J.; Muhammad, F. *Tetrahedron Lett.* **1965**, *35*, 625.

(24) For additional data see: Maddox, A. F.; Rheingold, A. L.; Golen, J. A.; Scott, K., W.; Nataro, C. *Inorg. Chim. Acta* **2008**, *361*, 3283–3293.

(25) Schuecker, R.; Weissensteiner, W.; Mereiter, K. *Acta Crystallogr.* **2011**, *E67*, m1379–m1380.

(26) (a) Boogers, J. A. F.; Sartor, D.; Felfer, U.; Kotthaus, M.; Steinbauer, G.; Dielemans, B.; Lefort, L.; de Vries, A. H. M.; de Vries, J. G. In *Asymmetric catalysis on industrial scale*; Blaser, H.-U., Federsel, H.-J., Eds.; Wiley-VCH: Weinheim, Germany, 2010; pp 127–150. (b) Li, S.; Zhu, S.-F.; Zhang, C.-M.; Song, S.; Zhou, Q.-L. *J. Am. Chem. Soc.* **2008**, *130*, 8584–8585.

(27) Li, S.; Zhu, S.-F.; Xie, J.-H.; Song, S.; Zhang, C.-M.; Zhou, Q.-L. *J. Am. Chem. Soc.* **2010**, *132*, 1172–1179.

(28) In our first report[12b] some product absolute configurations were given erroneously, and these require correction. In Table 1 the product configurations should read *S* for substrates **6** and **7** and in Table 2 2*S*,4*S* for substrate **9**.